

Simple water vapor sampling for stable isotope analysis using affordable valves and bags

Adrian Dahlmann¹, John D. Marshall², David Dubbert¹, Mathias Hoffmann¹ and Maren Dubbert¹

¹Isotope Biogeochemistry and Gas Fluxes, Leibniz Centre for Agricultural Landscape Research (ZALF), Müncheberg, 15374, Germany

²Department of Earth Sciences, University of Gothenburg, Gothenburg, 405 30, Sweden

Correspondence to: Adrian Dahlmann (adrian.dahlmann@zalf.de)

Abstract. Water stable isotopes are commonly used in hydrological and ecological research. Until now, most measurements of soil or plant water isotopes have been made by taking a sample from the field and extracting its water in the laboratory. More recently, samples have been collected with gas-permeable membranes (GPM) and measured in the field. These new methods, however, present challenges in achieving high-resolution measurements across multiple sites since they require significant effort and resources. Gas bag sampling offers the advantage of non-destructive, cost-efficient, easy-to-perform measurements without the need to bring a Cavity Ring-Down Spectroscopy (CRDS) analyzer into the field. We used gas-permeable membranes to extract samples of water vapor from the soil, which were then stored in multi-layer foil bags until analysis. The bags were modified with home-made connections to reduce leakage and simplify gas transfers. The bags were tested using laboratory standards to determine their maximum storage time, potential memory effects, and reusability. The storage experiment with new bags demonstrated the ability to store water vapor samples for up to 7 days while maintaining mostly acceptable trueness for $\delta^2\text{H}$, and acceptable to questionable trueness for $\delta^{18}\text{O}$. Trueness was defined as mean difference between the measured and known water vapor placed into the bags and precision by the standard deviation of replicate measurements. The memory experiment using new bags revealed that the influence of previous samples increased with duration of storage. In both experiments, the light standards seemed to result in less accuracy. The reuse experiment confirmed that the bags can be filled repeatedly, provided they are used for similar sample lines and flushed 10 times with dry air. To demonstrate bag applicability in the field, we compared measurements of stored samples to measurements made directly in the field. Storing beyond 24 hours needs further investigation but appears promising. With new gas bags up to 24 hours of storage, we found accuracies of $0.2\text{ ‰} \pm 0.9$ for $\delta^{18}\text{O}$ and $0.7\text{ ‰} \pm 2.3$ for $\delta^2\text{H}$. When the bags were reused and stored up to 24 hours, they yielded accuracies of $0.1\text{ ‰} \pm 0.8$ for $\delta^{18}\text{O}$ and $1.4\text{ ‰} \pm 3.3$ for $\delta^2\text{H}$. The proposed system is simple, cost-efficient, and versatile for both lab and field applications, however, case-specific testing is necessary given the remaining uncertainties.

36 **1. Introduction**

37 Water stable isotope measurements are used in a variety of scientific fields, particularly in
38 hydrology, ecohydrology, and meteorology, which focus on aspects of the water cycle. The
39 primary isotopes involved are ^{18}O and ^2H (e.g., Gat 1996; Mook 2000), described as $\delta^{18}\text{O}$ and
40 $\delta^2\text{H}$ relative to the most abundant isotopes, ^{16}O and ^1H (Sodemann, 2006). They serve to
41 investigate processes such as infiltration and groundwater recharge (e.g. Séraphin et al., 2016),
42 evaporation (e.g. Rothfuss et al., 2010), or the plasticity of root water uptake under stress (e.g.
43 Kühnhammer et al., 2021; Kühnhammer et al., 2023).

44 Traditionally, the isotopic composition of soil and plant water has been measured through
45 destructive sampling of soil cores or sampled plant material, followed by water extraction e.g.
46 via cryogenic extraction (see method summary Orlowski et al., 2016a) and measured with
47 isotope ratio mass spectrometry (IRMS) analyzers (West et al., 2006; Sprenger et al., 2015).
48 The development of smaller and less expensive cavity ring-down spectroscopy (CRDS)
49 analyzers has led to an increase in potential applications, including, e.g., in situ measurements
50 using gas permeable membranes (Rothfuss et al., 2013; Volkmann and Weiler, 2014; Volkmann
51 et al., 2016; Kübert et al., 2020; Landgraf et al., 2022). Direct measurements are a viable
52 alternative to classic destructive techniques, especially in small plots, as among other benefits
53 (e.g. high frequency measurements) they avoid repeated destructive sampling. However, direct,
54 continuous in situ field setups are very cost-intensive, technically challenging and require a
55 permanent power supply in the field as well as strong expertise to maintain. Moreover, direct
56 in situ field setups require full-time operation of one laser spectrometer (e.g. a CRDS) each,
57 whereas a vapor storage method could be operated with one CRDS for several field setups. To
58 allow an expansion to a wider set of potential study areas and increase the number of absolute
59 study areas maintainable, scientists are recently trying to develop new simplified sampling
60 systems. This includes capturing soil moisture as water vapor for subsequent laboratory analysis
61 (e.g. Havranek et al., 2020; Magh et al., 2022; Herbstritt et al. 2023). To do so, primarily glass
62 bottles or gas sampling bags with various fittings are used, which cost from ~1-200 euros per
63 container. The advantages of these methods include the ability to quickly measure stored
64 samples at elevated temperatures relative to the source in a temperature-stable laboratory
65 environment. In addition, multiple sample containers can be filled at once in the field, which
66 allows for the simultaneous measurement of multiple probes, and sampling can generally be
67 performed at a much faster rate. These simplified and more affordable systems could therefore
68 increase the number of studies on water stable isotopes and provide new insights in research by
69 increasing the number of possible experimental sites and samples.

70 In this study, we investigated the use of multi-foil bags with septum valves. Our investigation
71 focused on exploring the potential of these commercially available but affordable bags for a
72 wider range of applications (~ 20€ per bag plus ~ 15€ for the connection). To ensure easy and
73 reliable bag filling and measurement, we built an additional connection and a portable dry air
74 supply box system for easy field measurement. We tested the prepared bags in several
75 experiments in the laboratory using defined standards and, in the field, using comparison to in
76 situ measurements with a CRDS. The focus was to investigate storage capability as well as
77 possible isotopic fractionation effects due to exchange with the inner surface of the bags. Five
78 different experiments were performed: i) a storage experiment up to 7 days, ii) a memory
79 experiment without sample storage and two quite different standards, iii) a memory experiment
80 with 1 day of storage of the initial standard followed by sample replacement exploring duration
81 effects on memory setting and, iv) a field filling and bag reuse experiment to compare the bag
82 measurements with in situ CRDS measurements. These were followed by v) a gas bag
83 measurement sequence over a full cultivation period. These results allowed us to find a simple
84 approach to using septum-based gas bags for field measurements of water stable isotopes.

85 **2. Material and methods**

86 **2.1 Study area and basics of water stable isotope measurements**

87 The laboratory experiments were carried out at the Leibniz Centre for Agricultural Landscape
88 Research (ZALF). The field experiments took place at the AgroFlux experimental platform of
89 ZALF (see Dahlmann et al., 2023 for further details), located in the northeast of Germany, near
90 Dedelow in the Uckermark region (N 53°22'45", E 13°47'11"; ~50-60 m a.s.l.).

91 During the experiments, the $\delta^2\text{H}$ and $\delta^{18}\text{O}$ values were recorded using a CRDS analyzer (L2130-
92 i, Picarro Inc., Santa Clara, CA, USA). The hydrogen and oxygen stable isotopes in the sampled
93 water vapor ($\delta^2\text{H}$ and $\delta^{18}\text{O}$) are given in per mil (‰), relative to the Vienna Standard Mean
94 Ocean Water (VSMOW) using δ -notation (Eq. 1; Craig, 1961).

$$95 \quad \delta = \left(\frac{R_{\text{sample}}}{R_{\text{VSMOW}}} - 1 \right) \times 1000 \text{ [‰]} \quad \text{Eq. 1}$$

96 During all experiments, water stable isotope signatures ($\delta^2\text{H}$ and $\delta^{18}\text{O}$ in ‰) were measured
97 with the method of Rothfuss et al. (2013), using gas permeable membranes (GPM, Accurel GP
98 V8/2HF, 3M, Germany; 0.155 cm wall thickness, 0.55 cm i.d., 0.86 cm o.d.; e.g. as used in
99 Kübert et al., 2020 or Kühnhammer et al., 2021). In the laboratory experiments, we attached
100 two membranes to the cap of a 100 ml glass bottle with two stainless steel fittings (CUA-2, Hy-

101 Lok D Vertriebs GmbH, Germany) to directly measure standard water vapor and to fill the bags.
102 The glass bottle was filled with approx. 60 - 80 ml of standard water. The first membrane was
103 submerged in the standard water, where it bubbles the dry air through, resulting in equilibration
104 of water vapor in the headspace with the standard water. The second membrane, in the
105 headspace, collects saturated sample air and supplies it to the analyzer. Both membranes were
106 sealed with adhesive. The second membrane (< 5 cm) served as a safety mechanism to prevent
107 liquid water from entering the tubing.

108 A gas cylinder was used to induce dry gas at a low flow rate of 50 - 80 ml per minute (257-
109 6409, RS Components GmbH, Germany). We ensured that the isotopic signature of the vapor
110 would be at equilibrium with liquid water at this flow rate. We tested flows from the minimum
111 required for Picarro operation (approx. 35 ml/min) to 300 ml/min and found consistent results
112 up to 100 ml/min. At the lower flow rates, the water vapor passing through the membrane
113 reached isotopic thermodynamic equilibrium (Majoube, 1971; Horita and Wesolowski, 1994).
114 In the field experiments, we used approx. 12 cm membranes (comparable to soil GPM in e.g.
115 Kühnhammer et al., 2021) attached to PTFE tubing to sample the four different soil depths (see
116 section 2.7). The in situ method was likewise based on the measurement of water vapor with
117 the assumption that the vapor was in isotopic equilibrium with the liquid water surrounding the
118 sample probe (Rothfuss et al., 2013). Finally, the isotopic fractionation was calculated as a
119 function of the temperature (T) at the phase transition using equations based on Majoube
120 (1971).

121 The water vapor from the standards and soil was then either transferred immediately to the
122 CRDS analyzer and measured directly or it was stored in the gas bags and measured later. In
123 laboratory experiments I, II and III, the temperatures were around 20°C during filling and
124 around 24°C during storage and bag measurement to avoid condensation. In field experiments
125 IV and V, great care was taken to measure the bags at elevated temperatures relative to the
126 source temperatures.

127 In laboratory experiments, calibration was performed by measuring the described glass bottles
128 before the start of the measurement and the used standard during and after the experiment for
129 drift correction. In field experiments, the standards covering the expected sampled isotopic
130 range were filled into bags and treated similarly to the samples. Calibration was then performed.

131

132

133 **2.2 Storage and sampling design**

134 **2.2.1 Gas bag design**

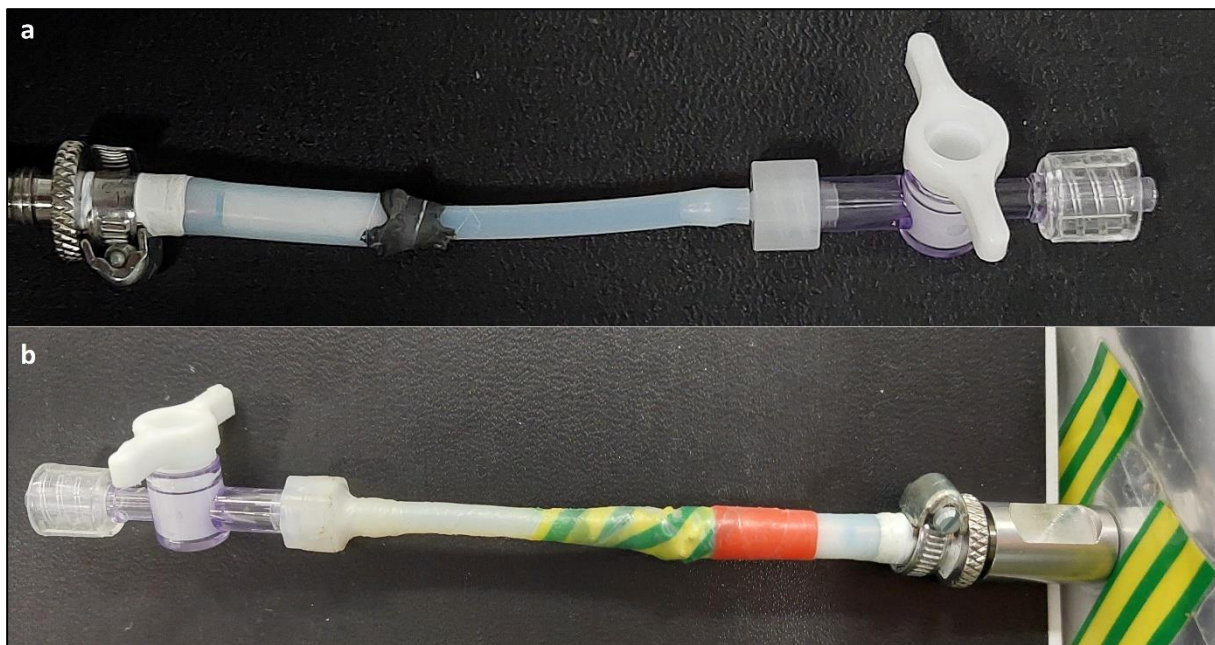


Figure 1: Self-constructed luer-lock connector with the splice exposed (a) and stabilized with tape attached to the bag on the right (b).

135 The sampling and measurement concept was intended to be as simple as possible, while still
136 providing high accuracy and precision. Water vapor samples were stored in 1-L multi-layer foil
137 bags with a septum-based valve (11 Multi-Layer Foil Bags with stainless steel fitting, Sense
138 Trading B.V., Netherlands; see Table S1 for more details; Sense Trading B.V., 2024). The
139 stainless steel 2-in-1 fitting combined the valve and septum, with the septum acting as a seal,
140 allowing air to flow around it when the valve was open, and sealing when the valve was closed.
141 As recommended by the manufacturer, care was taken when filling the bags to ensure that the
142 maximum volume did not exceed 90% of nominal capacity, which could cause material
143 damage. The connection (Fig. 1) was built to easily attach the bags with the sample setup. It
144 consisted of two short PTFE tubes (PTFE-tubing, Wolf-Technik eK, Germany) and an
145 additional luer-lock stopcock (1-way Masterflex™ Stopcocks with Luer Connection, Avantor,
146 USA). A hose clamp (TORRO SGL 5mm, NORMA Group Holding GmbH, Germany) was
147 used to directly connect a quarter-inch tube to the valve and the other 4 mm tube was glued into
148 the quarter-inch tube using 2-component-adhesive (DP8005, 3M Deutschland GmbH,
149 Germany). Since the adhesive contact with the PTFE tube could break under tension and cause
150 leakage, we wrapped electrical insulation tape around the splice to reinforce the connector. This
151 tape was not essential for sealing. Then, a luer-lock connection (LF-1.5NK-QC, GMPTEC
152 GmbH, Germany) was used to connect the luer-lock stopcock.

153 **2.2.2 Sampling design**

154 For the 1) direct standard measurements, the sample generated was passed directly to the laser
155 spectrometer to determine its isotopic signature. Since the laser spectrometer only has a flow
156 rate of approx. 35 to 40 ml per minute, an open split was added to ensure a constant flow and
157 to avoid pressure differences. Flow at the open split was measured continuously to ensure that
158 no ambient air could flow back. A 5-minute average was taken at the end of a minimum 10-
159 minute measurement for direct standard measurements.

160 For the 2) field measurements, the membranes were installed at the four different depths of 5
161 cm, 15 cm, 45 cm and 150 cm, and water vapor was transported out of the soil using 4 mm
162 PTFE tubing. The open ends were fitted with Luer connectors for later connection of gas sample
163 bags and the dry air supply. To protect these open ends from environmental influences,
164 waterproof outdoor boxes were installed 20 to 30 cm above the ground (outdoor.case type 500,
165 B&W International GmbH, Germany). Cable glands were used to keep the boxes watertight
166 (PG screw set, reichelt elektronik GmbH, Germany).

167 A separate box was built to
168 supply pressurized dry air
169 to the measuring system
170 during the field
171 experiments (Fig. 2). This
172 contained a pump
173 (NMP850KPDC-B, KNF
174 DAC GmbH, Germany)
175 including a power supply
176 (DPP50-24, TDK-Lambda
177 Germany, Germany),
178 which could transport the

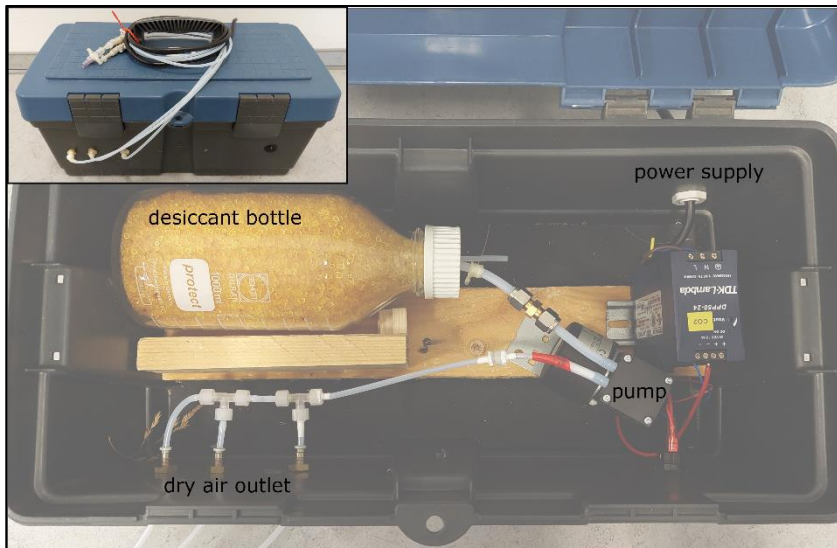


Figure 2: Self-constructed box for field dry air supply (top left) including a bottle with desiccant, power supply and a pump for up to three dry air outlet lines.

179 dry air in three tubes simultaneously through up to three sample lines. The air is ambient air
180 which is dried by a desiccant (Silica Gel Orange, Carl Roth GmbH + Co. KG, Germany)
181 contained in a 1-liter bottle (Screw top bottle DURAN®, DWK Life Science, USA). To regulate
182 the flow of individual sample lines, fixed valves were used (AS1002F-04, SMC Deutschland
183 GmbH, Germany). The dry air supply box was tested prior to our experiments by measuring
184 the outlet concentration of the dry box over the course of 1 day. However, the use of such a
185 system should always be tested for the specific application, as a very high flow rate combined
186 with very humid air could greatly affect the duration of possible use. During the experiments,

187 we periodically tested the water concentration before and after the field campaigns and could
188 not detect any increase after 1 day in the field. The water concentration of the dry air produced
189 was approx. 200 ppm.

190 **2.3 Laboratory standards**

191 The water stable isotope measurements were
192 calibrated against six water vapor standards
193 (see Table 1) that were manually measured
194 during the experiments. Temperature (T) was
195 recorded continuously every 30 seconds with a
196 thermometer (EBI 20-TH1, Xylem Analytics
197 Germany Sales GmbH & Co. KG, Germany)

Table 1: Liquid water standards used during the experiments.

Standard	$\delta^{18}\text{O}_{\text{liquid}} [\text{\textperthousand}]$	$\delta^2\text{H}_{\text{liquid}} [\text{\textperthousand}]$
L22	- 19.9	- 148.1
M22	- 9	- 63.3
H22	2	12.9
L23	- 16	- 108.2
M23	- 9.2	- 63.9
H23	- 1.3	- 32

198 placed directly next to the standard container. This allowed us to measure the standards in the
199 vapor phase and infer the values in a liquid phase at equilibrium (Sec. 2.5). Of the six standards
200 with different δ values, approx. 60 ml were filled into the prepared 100 ml standard bottles as
201 described in section 2.1 and measured directly on the CRDS.

202 **2.4 Experimental design**

203 **2.4.1 Experiment I: Storage duration**

204 In our storage experiment, we tested our gas sample bags for water vapor storage using water
205 sources of known isotopic composition. New bags, including the self-made connections, were
206 prepared to eliminate any production artifacts. Each bag was cycled with dry air, filled, and
207 emptied five times in a row. Following this preparation, five bags per storage period were filled
208 with two standards, L22 and M22 (15 min. at 50 ml/min.).

209 Upon filling, the gas bags were promptly measured to ensure that no isotopic fractionation
210 occurred during the filling process. Subsequently, the gas bags were stored in the laboratory for
211 three storage durations - 1 day, 3 days, and 7 days. After the designated storage periods, the
212 samples were measured for 4 to 5 minutes, and a stable 2-minute average was recorded.

213 **2.4.2 Experiment II: Memory**

214 We conducted two memory tests, maintaining a consistent methodology similar to that
215 employed during the storage experiment, both utilizing five newly prepared bags per standard.
216 In the first test, we followed a structured sequence: we filled gas bags with the initial standard,
217 emptied them, and switched to the opposite standard and refilled the bags. We repeated the
218 process three times (fill, measure, empty) with the opposite standard until our measurements

219 fell within the required acceptable range (defined in 2.5). In the first experiment, L23 was used
220 as the initial standard and H23 as the opposite standard, in the second experiment, the standards
221 were used in reverse order.

222 **2.4.3 Experiment III: Memory test with storage**

223 This laboratory experiment was conceived after we observed the effect of a short delay on
224 memory in Experiment II. We followed a similar procedure except that the initial standard L22
225 was allowed to stand in the bags for 1 day prior to replacement with the second standard H22.
226 We then proceeded with the second standard following the repeated steps (fill, measure, empty)
227 until our measurements fell within the acceptable range again. Between the second and third
228 measurement cycle, the experiment was interrupted due to the long duration (1h) of each
229 measurement cycle and continued the next day (after 15.5 hours). The bags were left empty
230 during this second night to avoid any effects. Due to the length of each measurement cycle, we
231 used 3 repetitions during the experiment.

232 **2.4.4 Experiment IV: Field filling and bag reuse**

233 To validate results gained during the laboratory experiments under field conditions, we
234 compared measurements using the gas bags with direct in situ CRDS measurements. To do so,
235 we conducted two measuring campaigns, the first using new bags and the second using reused
236 bags. During the first one, we focused on the applicability of bag filling in the field by
237 comparing direct measurements of the soil water isotopes with the CRDS in the field
238 measurement of bagged samples. In the second campaign, we again compared direct field
239 measurements to bagged measurements, but this time using re-used bags measured in the
240 laboratory within 24 hours. To exclude any memory effects, as we saw in experiment III, the
241 reused bags were flushed 10 times with dry air (approx. 10 x 10 min). Identical sample bags
242 were utilized for the identical sample probe to minimize changes in isotopic composition and
243 reduce the impact of memory effects. During each of the two measurement campaigns, a total
244 of 48 samples were collected at four different depths: 5 cm (n = 14), 15 cm (n = 13), 45 cm (n
245 = 7), and 150 cm (n = 14). Due to low soil permeability, the depth of 45cm could only be
246 sampled during one measurement campaign, resulting in only 7 samples. Dry carrier gas was
247 passed through the home-built membrane soil probes at a flow rate of approx. 50 ml per minute.
248 First, we connected the CRDS to the outlet valve to determine the time required to reach a
249 steady-state value (compared to e.g. Kühnhammer et al., 2021). Subsequently, a 2-minute
250 average was recorded at the end of a 15-minute measurement for comparison with the
251 subsequent bag measurement. Second, we connected the bags and filled them for 15 minutes

252 (approx. 750 mL). The temperature at the sampled soil depth (TEROS 21, Meter Group, USA)
253 was logged using a datalogger (CR1000, Campbell Scientific Ltd., Germany) at 20-minute
254 averages and used to correct for equilibrium fractionation. Furthermore, it was used to
255 determine the saturated water concentration to control the concurrent measured concentration
256 in the probe.

257 **2.4.5 Experiment V: Observation over a full cultivation period**

258 The field applicability test was followed by gas bag sampling and subsequent water stable
259 isotope analyses in the laboratory for the same soil depths during a full winter wheat cropping
260 period (variety: "Ponticus"; sowing: September 26, 2022; harvest: July 18, 2023). We measured
261 once a month during the winter and once a week starting in the spring resulting in 18
262 measurement campaigns using only our gas bags. As was the case with experiment IV, identical
263 sample bags were used for the identical sample probes throughout all campaigns. Sample bags
264 were replaced with new ones if they were damaged. To provide context for the soil isotopic
265 data, additional precipitation samples were collected at the site over a two-year period.

266 **2.5 Calculation of isotope ratios, evaluation of uncertainty and data correction**

267 The isotope signatures of the collected water vapor water sample were converted to liquid water
268 isotope signatures using Majoube's method (Majoube, 1971). This conversion was based on
269 equilibrium fractionation at the source temperature T [K] (Eq. 2 and 3).

270

271
$$\delta_{liquid} = (\delta_{vapor} + 1000) \times \alpha^+ - 1000 \quad \text{Eq. 2}$$

272

273
$$\ln \alpha^+ = \left(a \frac{10^6}{T^2} + b \frac{10^3}{T} + c \right) \times 10^{-3} \quad \text{Eq. 3}$$

274

275 The equilibrium fractionation factor α^+ was determined based on Majoube's (1971)
276 experimental results, using the coefficients a, b and c (a = 1.137, b = -0.4156 and c = -2.0667
277 for ^{18}O and a = 24.844, b = -76.248 and c = 52.612 for ^2H).

278 To assess the uncertainty of our laboratory measurements, we calculated z-scores for each
279 sample and water stable isotope ($\delta^{18}\text{O}$ and $\delta^2\text{H}$). Z-scores indicate the normalized deviation of
280 the measured water isotopic ratios from the known isotopic signature of the added water vapor,
281 and can be calculated following the method (Eq. 4) described by Wassenaar et al. (2012):

282

283
$$z-score = \frac{S - B}{\mu} \quad \text{Eq. 4}$$

284

285 Where S is the isotope signature ($\delta^{18}\text{O}$ or $\delta^2\text{H}$) measured with our gas bag, B is the benchmark
286 isotope signature and μ is the target standard deviation. To assess the performance of each
287 extraction method, we set a target standard deviation (SD) of 2‰ for $\delta^2\text{H}$ and 0.4‰ for $\delta^{18}\text{O}$
288 for measuring water vapor samples. The target SD was selected based on CRDS measurements
289 using the bag method and considering standard deviations from previous studies, such as those
290 by Wassenaar et al. (2012) or Orlowski et al. (2016a). A z-score < 2 represents an acceptable
291 range, a z-score between 2 and 5 describes the questionable range, and a z-score > 5
292 representing an unacceptable range (Wassenaar et al., 2012; Orlowski et al., 2016a).

293 **3. Results**

294 The experimental results will be described using the following figure design: the defined
 295 standard deviation will be shown as a dashed blue box in plots of the true water vapor isotope
 296 values, which will be predominantly shown on the left side. The acceptable z-scores are shown
 297 as a dashed black box and the questionable z-scores are shown as a black box, predominantly
 298 on the right side. Both standard deviation and z-scores were defined in section 2.5.

299 **3.1 Experiment I: Storage duration**

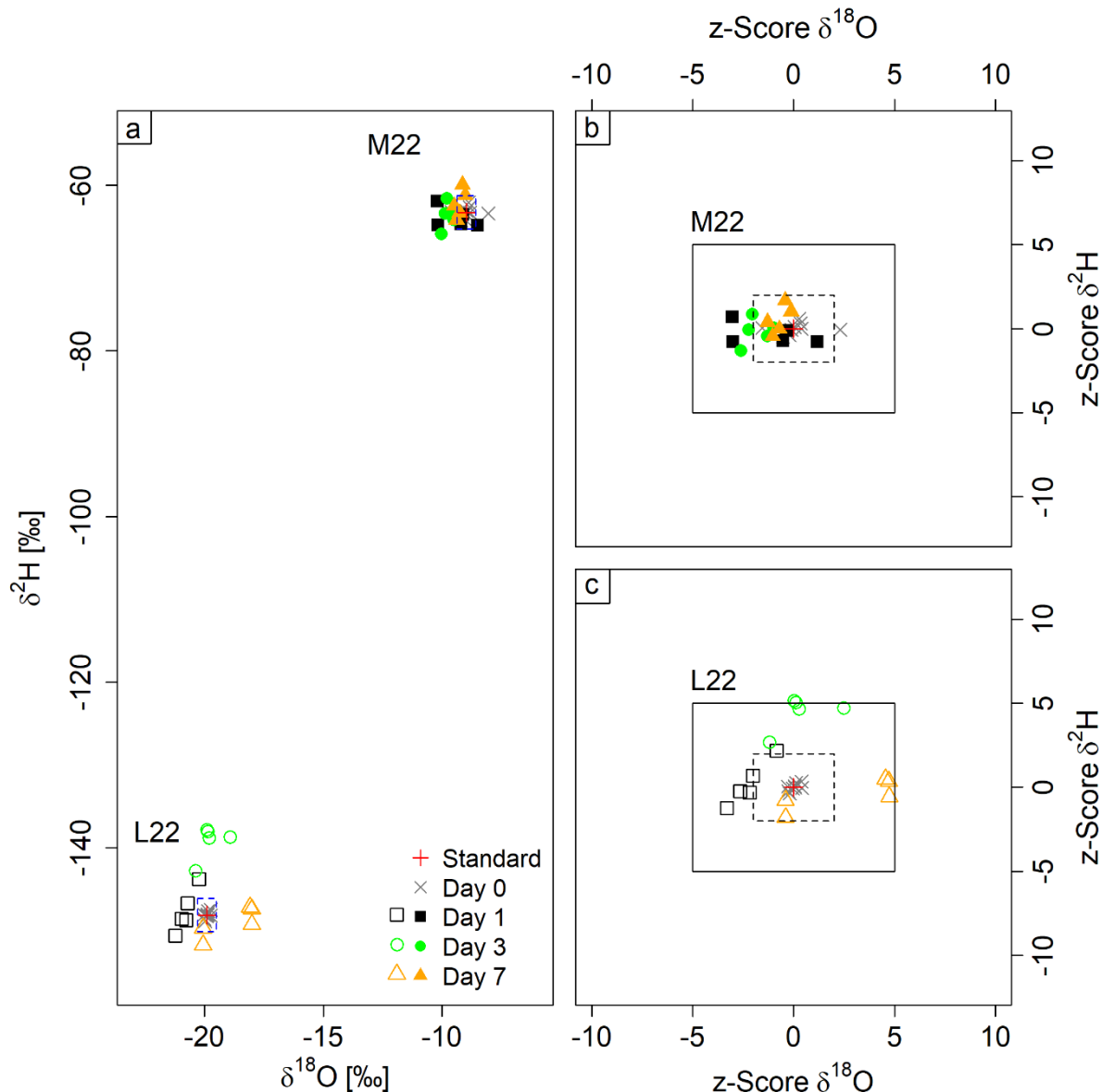


Figure 3: Dual isotope plots showing variation over several days of water-vapor storage in gas bags. The panel on the left shows results from both experiments (a) and those on the right show z-score plots for standard M22 (filled symbols, b) and L22 (open symbols, c). The black boxes describe the questionable range while the boxes delineated with a dashed line describes the acceptable range (b, c). The blue dashed line (a) describes the defined standard deviation for measurements.

300 Used laboratory standards, L22 and M22, spanned an isotopic range of -9.0 to -19.9 ‰ in $\delta^{18}\text{O}$
301 and -63.3 to -148.1 ‰ in $\delta^2\text{H}$ (Fig. 3a; filled symbols: M22, empty symbols: L22). On average,
302 the measured accuracies were $-0.7\text{ ‰} \pm 0.6\text{ ‰}$ $\delta^{18}\text{O}$ and $-0.1\text{ ‰} \pm 2\text{ ‰}$ $\delta^2\text{H}$ after 1 day, $-0.3\text{ ‰} \pm 0.6\text{ ‰}$
303 $\delta^{18}\text{O}$ and $4.3\text{ ‰} \pm 5.2\text{ ‰}$ $\delta^2\text{H}$ after 3 days and, $0.4\text{ ‰} \pm 1\text{ ‰}$ $\delta^{18}\text{O}$ and $0.1\text{ ‰} \pm 2\text{ ‰}$ $\delta^2\text{H}$ after 7 days of
304 storage (Table S2/S3). Except for one sample during the M22 experiment, the deviations from
305 the true standard values for these measurements were all within ± 0.4 for $\delta^{18}\text{O}$ and 2 ‰ for $\delta^2\text{H}$,
306 and thus no bias was associated with bag filling.

307 The experiment using standard M22 resulted in overall high accuracies for all measurements of
308 the three storage durations being $-0.5\text{ ‰} \pm 0.5\text{ ‰}$ for $\delta^{18}\text{O}$ and $0\text{ ‰} \pm 1.6\text{ ‰}$ for $\delta^2\text{H}$. In addition, no
309 trend in isotopic signature could be observed over storage duration for either $\delta^{18}\text{O}$ or $\delta^2\text{H}$.
310 Consequently, z-scores were either within the acceptable range or close to it, again with no
311 trend of decreasing accuracy over storage time.

312 The second storage test using L22, showed a lower accuracy due to lower precision for $\delta^2\text{H}$,
313 being $2.8\text{ ‰} \pm 4.9\text{ ‰}$, and $-0.1\text{ ‰} \pm 1.1\text{ ‰}$ for $\delta^{18}\text{O}$. However, no time trend was observed. The
314 decreased accuracy was mostly caused by the samples after 3 days, as all gas bags showed a
315 significant enrichment ($8.9\text{ ‰} \pm 2\text{ ‰}$ $\delta^2\text{H}$ on average). The higher inaccuracy after 3 days of
316 storage must be due to an error during the measurement, as accuracy improved again after 7
317 days. The overall higher scatter (particularly for $\delta^{18}\text{O}$), which has a different isotopic signature
318 than the ambient air, led to initial concern over potential exchange with ambient air. However,
319 we do not think that is likely as the visible scatter already appeared within 1 day of storage, was
320 not directed towards isotopic signatures of ambient air and did not increase over time. The z-
321 scores show acceptable values for $\delta^2\text{H}$ (except after 3 days) and more questionable values for
322 $\delta^{18}\text{O}$. The average z-score was 0.3 ± 2.7 for $\delta^{18}\text{O}$ and 1.4 ± 2.5 for $\delta^2\text{H}$.

323 **3.2 Experiment II: Memory**

324 In this experiment, the initial standard filled into the bags was L23, followed by cycles of filling
325 and emptying with standard H23. This standard sequence was reversed in the second part of the
326 experiment (initially H23, then cycles of L23). No clear memory effect was found in the first
327 part of the experiment (Fig. 4b), whereas a clear memory effect was observed after the first
328 filling (L1) of the second part of the experiment (Fig. 4c). However, this memory almost
329 disappeared in the next repetition (L2).

330 As depicted in Fig. 4 (a and c), except for L1, almost all measurements fell within the target
331 standard deviation for $\delta^{18}\text{O}$, while $\delta^2\text{H}$ values are more scattered. The same pattern can be seen
332 for the z-scores (Fig. 4 b and c). Three measurement points from L1 show unacceptable values,

333 while the remaining z-scores show acceptable or questionable values at the threshold of
 334 acceptable range.

335

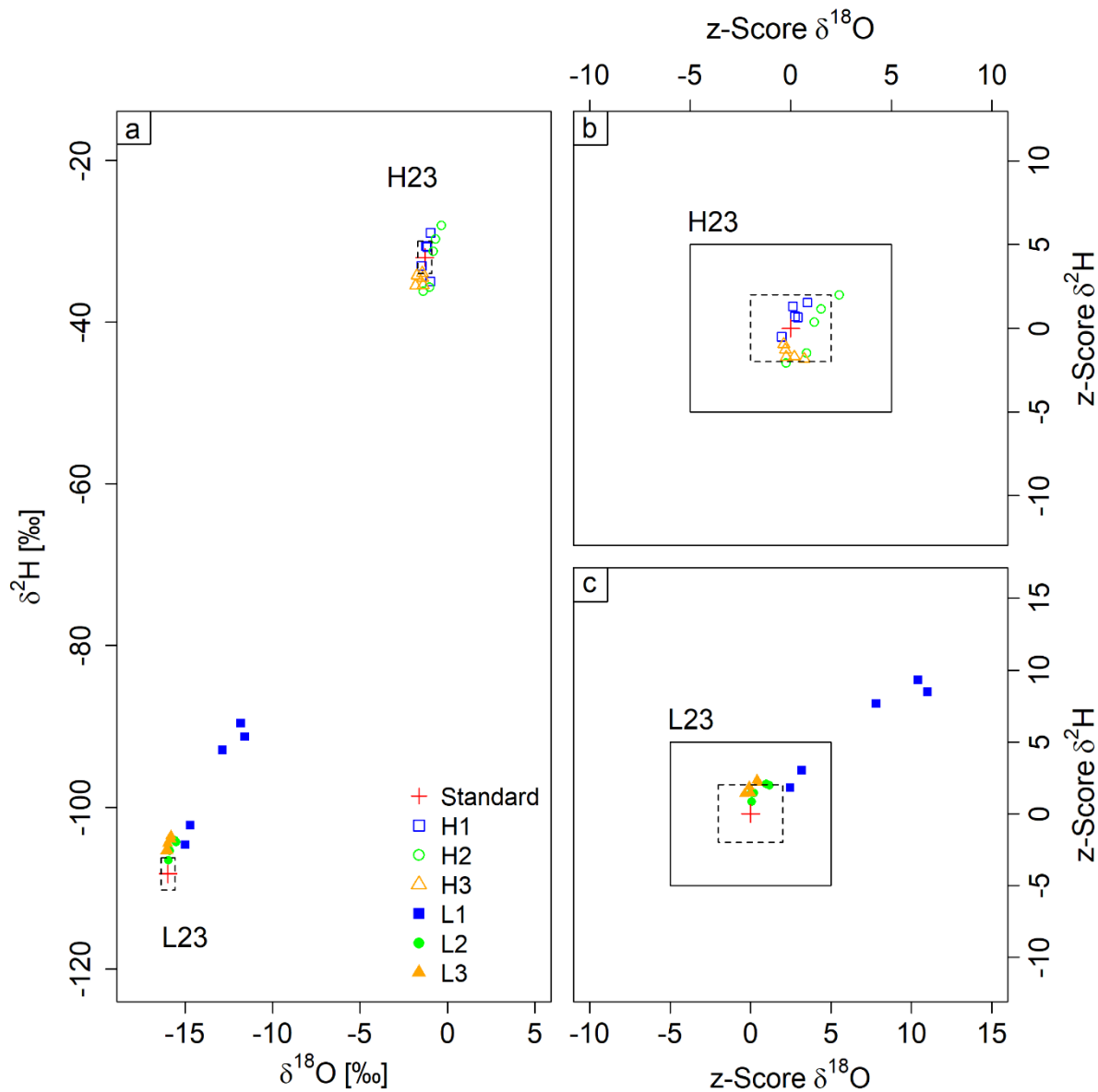


Figure 4: Memory experiment results with dual isotope plot for both experiments (a) and z-score plots for L23 to H23 (b) and H23 to L23 (c). The bags were filled first with standard H23, then repeatedly (1-3) with standard L23. The memory effect is evident only for measurement L1, the first to follow the change of source water vapor. The black box describes the questionable range while the scatter black box describes the acceptable range (b, c). The blue dashed line (a) describes the defined standard deviation for measurements.

336

3.3 Experiment III: Memory test with storage

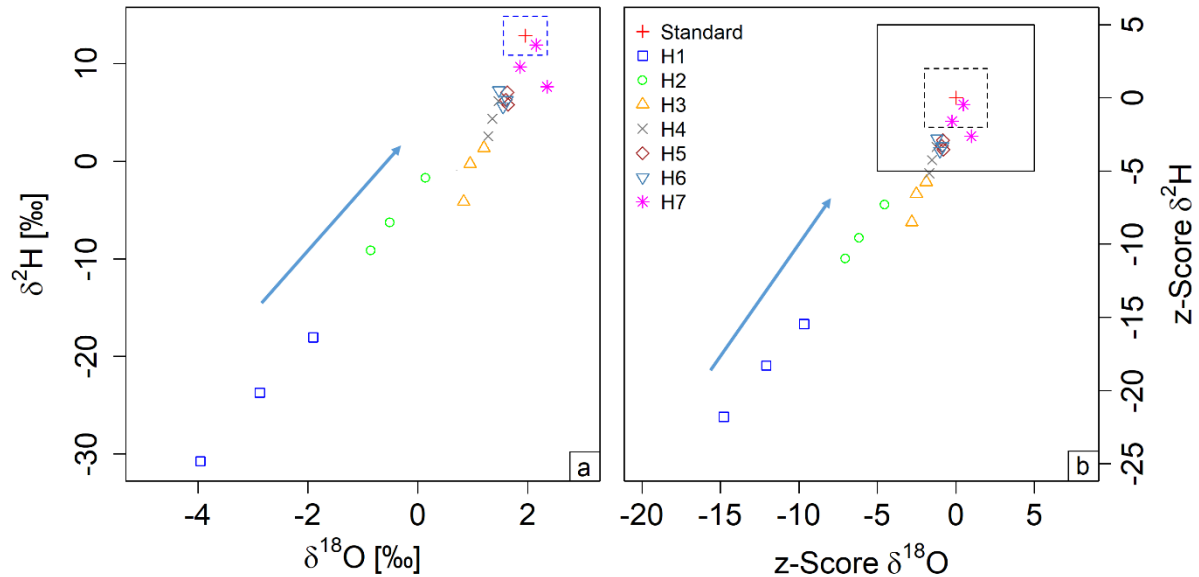


Figure 5: Memory test with storage experiment: dual isotope plot on the left (a) and z-score plot on the right (b). The red cross describes the target standard value. The blue dashed line (a) describes the defined standard deviation for measurements. The black box describes the questionable range while the dashed black box describes the acceptable range, based on our classification of z-values (b) (Sec. 2.5). The arrow indicates the direction from strong to weak memory effect.

No significant storage effect was observed over the 1-day storage period, and there was no noticeable difference between the two repetitions (mean difference between days: $0.4\text{‰} \pm 0.4\text{‰}$ $\delta^{18}\text{O}$ and $0.1\text{‰} \pm 1.9\text{‰}$ $\delta^2\text{H}$). However, when the water source was changed to H22, there was a clear memory effect of a magnitude up to $-4.9\text{‰} \pm 1$ in $\delta^{18}\text{O}$ and $-37\text{‰} \pm 6.4$ in $\delta^2\text{H}$ (Fig. 5 and Tab. 2). After filling with the opposite standard, H22, the first measurements (H1) revealed a low accuracy due to low precision and trueness, which was improved by around 50% with each repetition until the average result of H7 was close to the target standard value. The z-scores followed a similar trend from H1 to H5, gradually decreasing. Although H1 and H2 showed unacceptable z-scores for $\delta^{18}\text{O}$, and H3 fell within the questionable range, all subsequent measurements had z-scores within the acceptable range. The $\delta^2\text{H}$ z-scores follow a similar trend to the z-scores for $\delta^{18}\text{O}$, thus also indicating a clear memory effect. However, this effect persisted for more cycles in the case of $\delta^2\text{H}$. The measurements H1 to H3 were in the unacceptable range, while the results for H4 to H6 were questionable.

Table 2: Mean differences between measured and known isotopic signatures (S-B, eq. 4) of the different repetitions of the combined storage and memory experiment.

Repetition	Diff. $\delta^{18}\text{O}$ [‰]	Diff. $\delta^2\text{H}$ [‰]
H1	-4.9 ± 1	-37 ± 6.4
H2	-2.4 ± 0.5	-18.6 ± 3.7
H3	-1 ± 0.2	-13.9 ± 2.8
H4	-0.6 ± 0.1	-8.5 ± 1.8
H5	-0.3 ± 0	-6.5 ± 0.7
H6	-0.4 ± 0.1	-6.5 ± 0.9
H7	0.2 ± 0.3	-3.1 ± 2.2

358 **3.4 Experiment IV: Field filling and bag reuse**

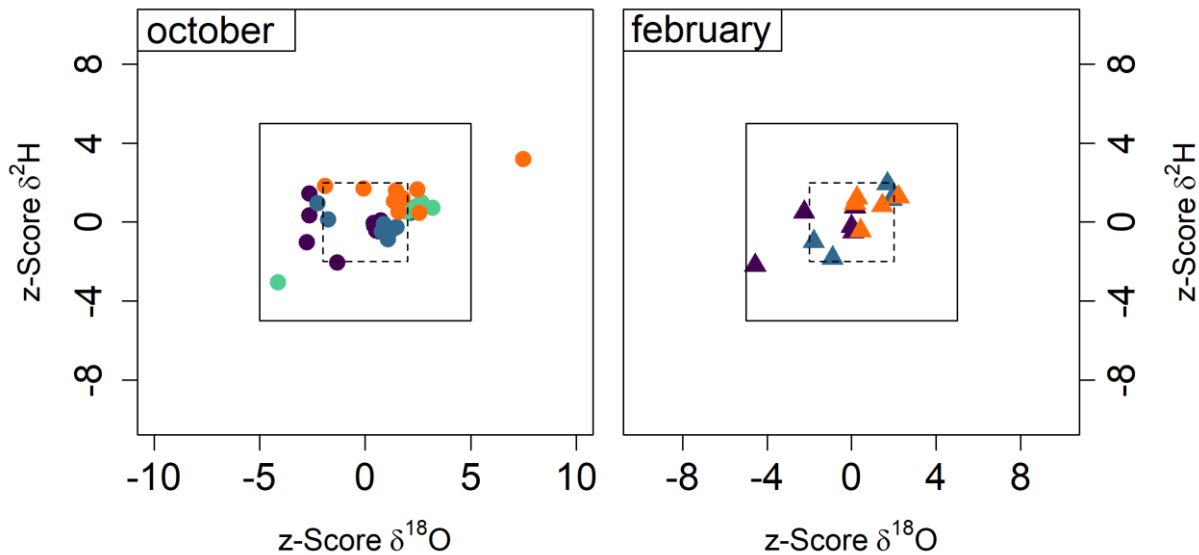


Figure 6: In October (left), in situ CRDS measurements were compared with bag measurements taken and measured directly after filling. In February (right), in situ CRDS measurements were compared with reused bags measured the next day in the laboratory (after 10 cycles of flushing with dry air).

359 To compare the measurements during the two campaigns and calculate the z-scores (Eq. 4), we
 360 considered the measured isotopic value made by the CRDS in the field as the benchmark value
 361 (B) and the measurements from the gas bags as the sample (S). The average difference between
 362 direct measurement and bag measurement was $0.2\text{ ‰} \pm 0.9$ for $\delta^{18}\text{O}$ and $0.7\text{ ‰} \pm 2.3$ for $\delta^2\text{H}$
 363 during the first sampling campaign in October, 2022 and $0.1\text{ ‰} \pm 0.8$ for $\delta^{18}\text{O}$ and $1.4\text{ ‰} \pm 3.3$
 364 for $\delta^2\text{H}$ for the second sampling campaign with reused bags in February, 2023 (Fig. 6). The
 365 deviation of the bag method from direct in situ measurements was thus mostly within the
 366 uncertainty range of the in situ method and yielded in highly accurate z-scores for $\delta^2\text{H}$.
 367 However, the $\delta^{18}\text{O}$ z-scores exhibit a larger scatter compared to $\delta^2\text{H}$, consistent with the results
 368 of the laboratory storage
 369 experiment (Exp. I).

Table 3: Mean differences between direct and bag measurement ($S-B$, eq. 4) of water stable isotopes ($\delta^{18}\text{O}$ and $\delta^2\text{H}$) and z-scores of the different depth during the two field experiments.

Depth [cm]	Diff. $\delta^{18}\text{O}$ [%]	Diff. $\delta^2\text{H}$ [%]	Z-score $\delta^{18}\text{O}$	Z-score $\delta^2\text{H}$
New bags				
5	-0.3 ± 0.6	-0.6 ± 1.9	-0.7 ± 1.6	-0.3 ± 1
15	0.2 ± 0.6	-0.2 ± 1.1	0.5 ± 1.6	-0.1 ± 0.6
45	0.6 ± 1	0.4 ± 2.9	1.4 ± 2.5	0.2 ± 1.5
150	0.8 ± 1	2.9 ± 1.6	1.9 ± 2.5	1.5 ± 0.8
Reused bags				
5	-0.5 ± 0.8	-0.6 ± 2.3	-1.3 ± 2.1	-0.3 ± 1.2
15	0.4 ± 0.7	2.13 ± 4.2	0.9 ± 1.8	1.1 ± 2.1
150	0.4 ± 0.4	2.5 ± 2.6	1 ± 0.9	1.2 ± 1.3

371 **3.5 Experiment V: Observation over a full cultivation period**

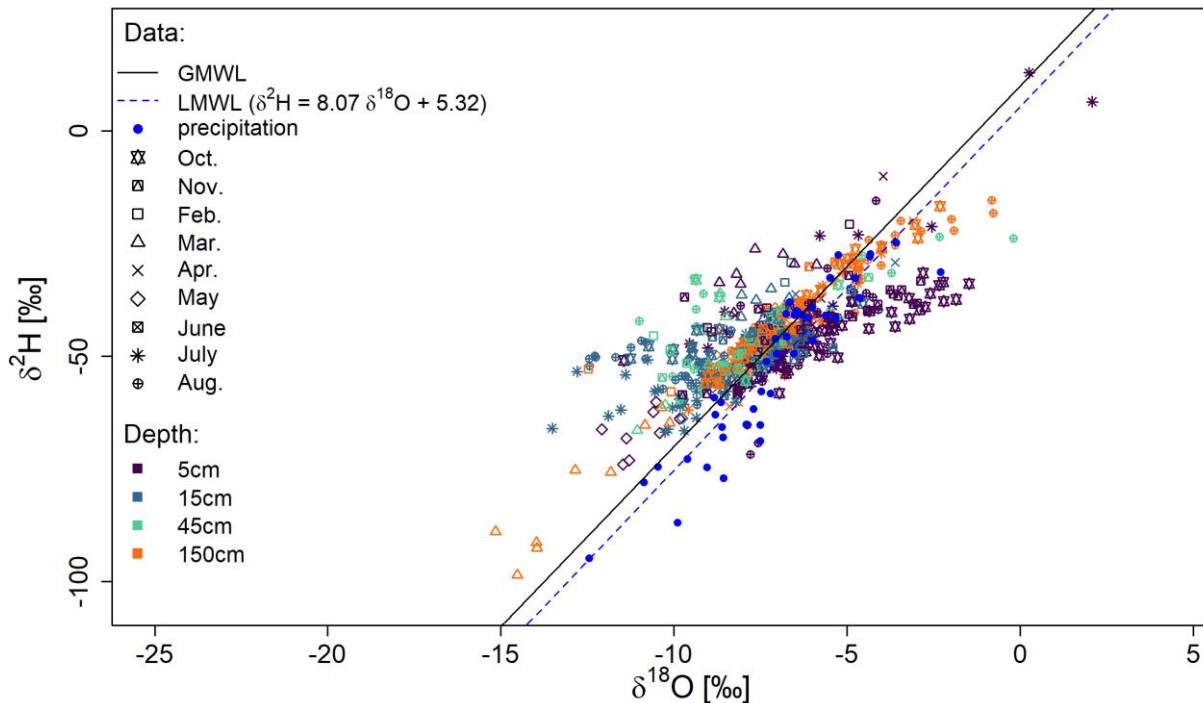


Figure 7: The dual isotope plot shows all 603 measurements taken during the cultivation period, including the Global Meteoric Water Line (GMWL; black line), the Local Meteoric Water Line (LMWL; blue dashed line) and the bag method measurements at 5, 15, 45 and 150 cm depth (purple, blue, green and yellow) during 9 different months.

372 Measurements of soil water isotope profiles over the full season (Fig. 7) revealed a wide range
 373 of isotopic signatures with 2.1 ‰ to -15.2 ‰ for $\delta^{18\text{O}}$ and 12.9 ‰ to -98.5 ‰ for $\delta^{2\text{H}}$. Of the
 374 623 measurements taken, 20 measurements or 3.2% had to be discarded due to damaged bags,
 375 filling errors, or condensation during the measurement and are therefore not shown (see
 376 "Handling Recommendations" in the supplement for further details). The isotopic signature of
 377 precipitation is represented by the local meteoric water line (LMWL), shown here for the period
 378 of September 2021 to September 2023. The LMWL is nearly parallel to the Global Meteoric
 379 Water Line (GMWL). In general, the measurements show isotopic signatures similar to
 380 precipitation immediately after rain events and a trend toward evaporative enrichment during
 381 droughts (see Fig. S1, supplement), but with distinct differences between months (e.g., Mar. vs.
 382 Oct., at the 5 cm depth). Overall, our findings from the field trial suggest a good agreement
 383 with the LMWL and are plausible in terms of seasonal variability.

384 **4. Discussion**

385 **4.1 Comparison to previous developments to store and measure water vapor**

386 In general, it is difficult to compare the different approaches to water vapor sampling for
387 isotopic analysis because they vary in complexity and application (e.g., storage time or price
388 per sample). However, our results for reused bag samples stored up to 24 hours are generally
389 comparable in accuracy to previous studies of water vapor storage. For example, the Soil Water
390 Isotope Storage System (SWISS) introduced by Havranek et al. (2020) showed a higher
391 precision during a 30-day storage period in a laboratory experiment ($\pm 0.5 \text{ ‰ } \delta^{18}\text{O}$ and ± 2.4
392 $\text{‰ } \delta^2\text{H}$). This result was followed by several experiments, which showed an actual precision of
393 0.9 ‰ and 3.7 ‰ for $\delta^{18}\text{O}$ and $\delta^2\text{H}$ in field applications with a storage time of 14 days (Havranek
394 et al., 2023). Their system is based on custom-made 750 ml glass vials with stainless steel
395 connections. Magh et al. (2022) developed the vapor storage vial system (VSVS), which is
396 based on crimp neck vials in combination with a PTFE/butyl membrane and has a similar
397 accuracy compared to our results after 1 day of storage, but, like the static vials used by
398 Havranek et al. (2020), requires a linear correction. Moreover, although the mean isotopic
399 composition remained the same throughout the measurement, it increasingly led to high scatter
400 of the measured isotopic signatures. Both systems are more difficult to handle during the
401 measurement compared to inflatable bags as they must be filled with the same amount of dry
402 gas mixture during the measurement due to the static volume of the glass vials.

403 A recent paper compared different types of affordable food storage bags for water vapor
404 sampling using standardized water with different isotopic signatures (Herbsttritt et al., 2023).
405 These authors conducted rigorous tests of diffusion tightness and inertness of various bag types.
406 They detected significant memory in all bag types, even after flushing with dry N_2 . To
407 circumvent these memory effects, they explored preconditioning of the bags with moist,
408 isotopically homogeneous air sample where the goal was not to eliminate the memory effect,
409 but to quantify and correct for it. After 1 storage day, the accuracies were $0.25 \text{ ‰ } \pm 0.41$ and
410 $0.41 \text{ ‰ } \pm 1.93$ for $\delta^{18}\text{O}$ and $\delta^2\text{H}$. This preconditioning resembles the pre-treatment of feathers
411 (Hobson et al., 1999) and hair (Ehleringer et al., 2020) to fill exchange sites with known water
412 vapor prior to analysis, followed by post-processing to remove the pre-treatment effect.

413 Our study differs from Herbsttritt et al. (2023) paper in several important ways. First, we have
414 used different bags, which are more expensive, but have better control over suppliers and better
415 description of specifications. Second, we have modified the valve inlets to the bags in a way

416 that simplified gas transfers and may reduce leakage. Third, we have suggested a means by
417 which multiple flushes of the bags with dry air may eliminate, or at least minimize, the memory
418 effect. Aside from the differences, we likewise identified a time-dependent memory effect,
419 which is consistent with the notion that some diffusion/adsorption process occurs over many
420 hours within the walls of the bag, setting an isotopic signal that requires multiple flushes to
421 remove. This time-dependent process does not seem to require slow flushing to reverse the
422 memory effect (Expt. IV). These results call for the automation of bag flushing protocols in
423 order to make these techniques routinely useful. Since the isotopic range in the experiment was
424 relatively narrow (< 20 ‰ for $\delta^2\text{H}$ between first and second sampling), we additionally
425 performed a small reuse experiment using two laboratory standards with higher differences in
426 isotopic signatures and 10 flushes with dry air (Fig. S2). As expected, results were unaffected
427 for both $\delta^{18}\text{O}$ and $\delta^2\text{H}$ directly after bag filling. While storage did not influence the $\delta^{18}\text{O}$
428 signature, a clear but consistent effect was visible after 1 day regarding $\delta^2\text{H}$, which, contrary to
429 the results of Herbstritt et al. (2023), did not increase over 3 days storage. Since this effect was
430 stable and we know the previous sample signature, this effect may be correctable as in the moist
431 conditioning approach described by Herbstritt et al. (2023) or erasable by increasing the number
432 of flushes. In conclusion, our results show comparable accuracy to other methods for storage
433 times of up to 24 hours, but the accuracy of long-term storage and high isotopic differences for
434 consecutive samples require further investigation.

435 To the best of our knowledge, a campaign of measuring soil water isotopes using gas bags over
436 an entire cultivation period, as shown in this study, has not been done before. However, such
437 studies have been done with other data collection techniques. For example, the isotopic
438 composition of water in surface soils can change significantly as evaporated soil vapor is
439 depleted in heavy isotopes, leaving the remaining soil water enriched in ^{18}O and ^2H (Dubbert
440 and Werner, 2018). This results in a wide range of isotopic signatures throughout the complete
441 cultivation season, as can be seen in the smaller slope compared to the LMWL in the upper soil
442 layer (Fig. 7). As expected, evaporative enrichment is evident following precipitation free
443 periods in the upper 5 cm depth (e.g. April period in Fig. S1), but not after the rainy winter
444 period. In contrast, there are only slight trends in evaporative enrichment at lower depths
445 (compare e.g. Sprenger et al., 2016).

446

447

448 **4.2 Limitations, future perspective and cost classification**

449 In the past, destructive measurements of soil water have relied predominantly on cryogenic
450 vacuum extraction (CVE). The accuracy of CVE can vary greatly for soil samples and is
451 associated with co-extraction of organic compounds, significantly interfering with the isotopic
452 quantification using CRDS (Orlowski et al., 2016b). In comparison, methods using in situ soil
453 or xylem probes based on gas-permeable membranes have been reported to be highly accurate
454 but complex to handle and set up (Volkmann and Weiler, 2014; Volkmann et al., 2016; Rothfuss
455 et al., 2013; Kübert et al., 2020). Therefore, efforts to combine destructive with in situ sampling
456 continue.

457 As highlighted above, recent studies showed that sampling of water vapor with subsequent
458 analysis in the laboratory is possible with both glass bottles and different types of bags. Glass
459 containers revealed the advantage of less material effects and higher diffusion tightness while
460 gas bags were easier to measure due to their flexible structure. Nevertheless, further
461 experiments should investigate the detected interaction of water samples within the gas bag
462 wall. For example, while the storage experiment I results for $\delta^2\text{H}$ were mostly accurate, we
463 observed higher uncertainty for $\delta^{18}\text{O}$. Here, the light standard proved to be slightly more
464 difficult to handle than the medium standard, while maintaining similar accuracy. At first
465 glance, this decrease in accuracy seems to be similar for experiment II (higher uncertainty of
466 light compared to heavy standard). In this experiment, a memory effect was expected given that
467 the previous sample was not removed between standard fillings. However, when the initial
468 standard was stored only briefly (minutes) before refilling with the opposite standard, as
469 planned in experiment II, no clear memory effect was observed. The three measurements
470 yielding unacceptable values were accidentally stored longer (45 min between filling and
471 measurement, see blue squares in Fig. 4), providing valuable insight into a memory effect
472 dependent on storage duration of the initial standard. Nevertheless, further studies should focus
473 on whether samples with isotopically lighter signatures or isotopic signatures outside of the
474 range tested in this study vary in accuracy when sampled and analyzed with the bag method.
475 Based on our observations in experiment II, experiment III deliberately combined memory with
476 storage resulting in a clear memory effect in the direction of the initial standard after 1 day of
477 storage for bags that were not subjected to a flushing procedure (such as described in Herbstritt
478 et al., 2024) before changing from one to the other standard. The observed number of refills
479 required in this experiment with the standard H22 after an initial fill with L22 to eliminate this
480 effect was used to guide our bag preparation strategy for bag reuse in the following experiment

481 IV. Unlike experiments I and II, this experiment tested only the direction from light to heavy
482 isotopes. Given the remaining uncertainty from experiments I and II concerning our light
483 standard performance, this should be revisited in future studies to test whether or not the
484 combined effect of memory and storage is stable over the desired isotope range. Finally, our
485 reuse experiment (IV) showed similar results to experiment I. Here, we proved that a
486 preconditioning of 10 dry air flushes between two bag sampling campaigns worked for
487 differences of up to 20 ‰ in $\delta^2\text{H}$ for consecutive samples, while a much higher difference of
488 76.2 ‰ revealed a memory effect of about 12 ‰ after 1 and 3 days of storage for $\delta^2\text{H}$ but not
489 for $\delta^{18}\text{O}$ (experiment S2). These results clearly show that the method provided good results for
490 our isotopic range in the field, but that further tests are required for experiments with a larger
491 range of isotope signatures particularly when considering use of this method for labelling
492 experiments. However, it should be noted that bags have never been tested for reuse with such
493 high isotopic differences, and some increase in uncertainty is to be expected due to the small
494 but present water transmission through the material. Considering this, the glass container used
495 in other methods may be superior for longer storage times, although e.g. Magh et al. (2022) also
496 recommended their method for storage times less than 3 days.

497 The cost of the commercial gas bags we used was relatively low compared to the total cost of
498 a typical field campaign. In perspective, the SWISS-System was clearly more expensive when
499 considering costs per container, while the other methods were less expensive per sample
500 container with 1-2€ but produced running cost (Magh et. al., 2022) or additional cost and effort
501 to attach the valve and built the final bag (Herbsttritt et. al., 2023). We have demonstrated that
502 commercially available bags meet the expected level of performance already, provided that
503 samples are stored up to 24h, they are flushed multiple times between uses, they are reused for
504 a relatively narrow range of isotopic signatures (in the case of $\delta^2\text{H}$) e.g. reusing the same bags
505 for the same sample probes, and that standards are taken through the whole sample collection,
506 transport, and analysis process. Following the conditions described, we were able to reliably
507 measure soil water over a full cultivation period under natural abundance conditions.

508 4. Conclusion

509 Our laboratory and field experiments have confirmed the reliability of soil membranes
510 combined with gas bags for in situ soil water vapor sampling and subsequent water stable
511 isotope analyses, provided the analysis occurs within 24h. The method is cost-efficient and easy
512 to handle, allowing for many future applications. We were able to demonstrate that both 1)
513 storage is possible and 2) memory effects caused by previous samples can be prevented by

514 appropriate preconditioning, allowing the gas bags to be reused. Regarding the isotopic
515 signature during the experiment, reuse is easier to carry out with smaller differences between
516 the consecutive samples in the bags. However, for larger differences in isotopic signatures, the
517 bags need to be handled differently, which needs to be further investigated (e.g. better flushing
518 between samples or no reuse). Through the field experiment (two campaigns with CRDS and
519 bag measurements), we were able to show that the bags could be used in our case with
520 accuracies of $0.23\text{‰} \pm 0.84\text{‰}$ $\delta^{18}\text{O}$ and $0.94\text{‰} \pm 2.69\text{‰}$ $\delta^2\text{H}$ for storage up to 24h. The possibility
521 to collect and store samples easily and without permanent power supply extends the usability
522 of water stable isotope measurements in the field.

523 **5. Data availability**

524 The data will be available in the BonaRes repository upon publication.

525 **6. Author contribution**

526 AD and MD designed the study. AD conducted experiments and analyzed the data. JM, DD,
527 and MH provided support for the experimental setup and analysis methods. AD prepared the
528 paper with supervision from MD and contributions from all co-authors.

529 **7. Competing interests**

530 The authors declare that they have no conflict of interest.

531 **8. Acknowledgements**

532 We acknowledge funding by ZALF Leibniz as well as the Leibniz association (ISO-SCALE
533 project; project number K444/2022). The authors wish to thank the Experimental Infrastructure
534 Platform (EIP) of ZALF and Linda Röderer for assisting with the field experiments.

535 **9. References**

536 Craig, H.: Standard for Reporting Concentrations of Deuterium and Oxygen-18 in Natural
537 Waters, *Science*, 133, 1833–1834, <https://doi.org/10.1126/science.133.3467.1833>, 1961.
538 Dahlmann, A., Hoffmann, M., Verch, G., Schmidt, M., Sommer, M., Augustin, J. and Dubbert,
539 M.: Benefits of a robotic chamber system for determining evapotranspiration in an erosion-
540 affected, heterogeneous cropland. *Hydrol Earth Syst Sc*, 27(21), 3851-3873,
541 <https://doi.org/10.5194/hess-27-3851-2023>, 2023.

542 Dubbert, M., and Werner, C.: Water fluxes mediated by vegetation: emerging isotopic insights
543 at the soil and atmosphere interfaces. *New Phytol*, 221(4), 1754-1763,
544 <https://doi.org/10.1111/nph.15547>, 2018.

545 Ehleringer, J. R., Bowen, G. J., Chesson, L. A., West, A. G., Podlesak, D. W., & Cerling, T. E.:
546 Hydrogen and oxygen isotope ratios in human hair are related to geography. *P Natl Acad
547 Sci-Biol*, 105(8), 2788-279, <https://doi.org/10.1073/pnas.0712228105>, 2008.

548 Gat, J. R.: Oxygen and hydrogen isotopes in the hydrologic cycle. *Ann Rev Earth Pl Sc*, 24(1),
549 225-262, <https://doi.org/10.1146/annurev.earth.24.1.225>, 1996.

550 Havranek, R. E., Snell, K. E., Davidheiser-Kroll, B., Bowen, G. J., and Vaughn, B.: The Soil
551 Water Isotope Storage System (SWISS): An integrated soil water vapor sampling and
552 multiport storage system for stable isotope geochemistry. *Rapid Commun Mass Sp*, 34(12),
553 e8783, <https://doi.org/10.1002/rcm.8783>, 2020.

554 Havranek, R. E., Snell, K., Kopf, S., Davidheiser-Kroll, B., Morris, V., and Vaughn, B.:
555 Lessons from and best practices for the deployment of the Soil Water Isotope Storage
556 System. *Hydrol Earth Syst Sc*, 27(15), 2951-2971, <https://doi.org/10.5194/hess-27-2951-2023>, 2023.

558 Herbstritt, B., Gralher, B., Seeger, S., Rinderer, M., and Weiler, M.: Discrete in situ vapor
559 sampling for subsequent lab-based water stable isotope analysis. *Hydrol Earth Syst Sc*,
560 27(20), 3701-3718, <https://doi.org/10.5194/hess-27-3701-2023>, 2023.

561 Hobson, K. A.: Tracing origins and migration of wildlife using stable isotopes: a review.
562 *Oecologia*, 120, 314-326, <https://doi.org/10.1007/s004420050865>, 1999.

563 Horita, J., and Wesolowski, D. J.: Liquid-vapor fractionation of oxygen and hydrogen isotopes
564 of water from the freezing to the critical temperature. *Geochim Cosmochim Ac*, 58(16),
565 3425-3437, [https://doi.org/10.1016/0016-7037\(94\)90096-5](https://doi.org/10.1016/0016-7037(94)90096-5), 1994.

566 Kübert, A., Paulus, S., Dahlmann, A., Werner, C., Rothfuss, Y., Orlowski, N., and Dubbert,
567 M.: Water stable isotopes in ecohydrological field research: comparison between in situ and
568 destructive monitoring methods to determine soil water isotopic signatures. *Front plant sci*,
569 11, 497124, <https://doi.org/10.3389/fpls.2020.00387>, 2020.

570 Kühnhammer, K., Dahlmann, A., Iraheta, A., Gerchow, M., Birkel, C., Marshall, J. D., and
571 Beyer, M.: Continuous in situ measurements of water stable isotopes in soils, tree trunk and
572 root xylem: Field approval. *Rapid Commun Mass Sp*, 36(5), e9232,
573 <https://doi.org/10.1002/rcm.9232>, 2021.

574 Kühnhammer, K., van Haren, J., Kübert, A., Bailey, K., Dubbert, M., Hu, J., Ladd, N. S.,
575 Meridith, L. K., Werner, C., and Beyer, M.: Deep roots mitigate drought impacts on tropical

576 trees despite limited quantitative contribution to transpiration. *Sci Total Environ*, 893,
577 164763, <https://doi.org/10.1016/j.scitotenv.2023.164763>, 2023.

578 Landgraf, J., Tetzlaff, D., Dubbert, M., Dubbert, D., Smith, A., & Soulsby, C.: Xylem water in
579 riparian willow trees (*Salix alba*) reveals shallow sources of root water uptake by in situ
580 monitoring of stable water isotopes. *Hydrol Earth Syst Sc*, 26(8), 2073-2092,
581 <https://doi.org/10.5194/hess-26-2073-2022>, 2022.

582 Marshall, J.D., Cuntz, M., Beyer, M., Dubbert, M., Kuehnhammer, K.: Borehole equilibration:
583 Testing a new method to monitor the isotopic composition of tree xylem water in situ. *Front
584 Plant Sci*, 11, 508657, <https://doi.org/10.3389/fpls.2020.00358>, 2020.

585 Magh, R. K., Gralher, B., Herbstritt, B., Kübert, A., Lim, H., Lundmark, T., and Marshall, J.:
586 Conservative storage of water vapour—practical in situ sampling of stable isotopes in tree
587 stems. *Hydrol Earth Syst Sc*, 26(13), 3573-3587, <https://doi.org/10.5194/hess-26-3573-2022>, 2022.

588 Majoube M. Fractionnement en oxygène 18 et en deutérium entre l'eau et sa vapeur. *J Chim
589 Phys*, 68, 1423-1436, <https://doi.org/10.1051/jcp/1971681423>, 1971.

590 Mook, W. G. (Eds.): Environmental isotopes in the hydrological cycle: principles and
591 applications. UNESCO/IAEA, Volume 1, Centre for Isotope Research, Groningen,
592 Netherlands, 280 pp., 2000.

593 Orlowski N., Pratt D.L., and McDonnell J.J.: Intercomparison of soil pore water extraction
594 methods for stable isotope analysis. *Hydrol Process*, 30(19), 3434-3449,
595 <https://doi.org/10.1002/hyp.10870>, 2016a.

596 Orlowski N., Breuer L., McDonnell J.J.: Critical issues with cryogenic extraction of soil water
597 for stable isotope analysis. *Ecohydrology*, 9(1), 3-10, <https://doi.org/10.1002/eco.1722>,
598 2016b.

599 Rothfuss, Y., Biron, P., Braud, I., Canale, L., Durand, J. L., Gaudet, J. P., Richard P., Vauclin
600 M., and Bariac, T.: Partitioning evapotranspiration fluxes into soil evaporation and plant
601 transpiration using water stable isotopes under controlled conditions. *Hydrol Process*,
602 24(22), 3177-3194, <https://doi.org/10.1002/hyp.7743>, 2010.

603 Rothfuss, Y., Vereecken, H., and Brüggemann, N.: Monitoring water stable isotopic
604 composition in soils using gas-permeable tubing and infrared laser absorption spectroscopy.
605 *Water resour res*, 49(6), 3747-3755, <https://doi.org/10.1002/wrcr.20311>, 2013.

606 Sense Trading B.V., personal communication, 2024.

608 Séraphin, P., Vallet-Coulomb, C., and Gonçalvès, J.: Partitioning groundwater recharge
609 between rainfall infiltration and irrigation return flow using stable isotopes: The Crau
610 aquifer. *J Hydrol.*, 542, 241-253, <https://doi.org/10.1016/j.jhydrol.2016.09.005>, 2016.

611 Sodemann, H. (Eds.): Tropospheric transport of water vapour: Lagrangian and Eulerian
612 perspectives. Swiss. ETH Zurich, No. 16623, 225 pp., ISBN 978-3832513849, 2006.

613 Sprenger M, Herbstritt B, Weiler M. Established methods and new opportunities for pore water
614 stable isotope analysis. *Hydrol Process.* 29(25), 5174-5192,
615 <https://doi.org/10.1002/hyp.10643>, 2015.

616 Sprenger, M., Leistert, H., Gimbel, K., and Weiler, M.: Illuminating hydrological processes at
617 the soil-vegetation-atmosphere interface with water stable isotopes. *Rev Geophys.*, 54(3),
618 674-704, <https://doi.org/10.1002/2015RG000515>, 2016.

619 Volkmann, T. H., and Weiler, M.: Continual in situ monitoring of pore water stable isotopes in
620 the subsurface. *Hydrol Earth Syst Sc.*, 18(5), 1819-1833, <https://doi.org/10.5194/hess-18-1819-2014>, 2014.

621 Volkmann, T. H., Haberer, K., Gessler, A., and Weiler, M.: High-resolution isotope
622 measurements resolve rapid ecohydrological dynamics at the soil-plant interface. *New
623 Phytol.*, 210(3), 839-849, <https://doi.org/10.1111/nph.13868>, 2016.

624 Wassenaar, L. I., Ahmad, M., Aggarwal, P., Van Duren, M., Pöltenstein, L., Araguas, L., and
625 Kurttas, T.: Worldwide proficiency test for routine analysis of $\delta^2\text{H}$ and $\delta^{18}\text{O}$ in water by
626 isotope-ratio mass spectrometry and laser absorption spectroscopy. *Rapid Commun Mass
627 Sp.*, 26(15), 1641-1648, <https://doi.org/10.1002/rcm.6270>, 2012.

628 West, A. G., Patrickson, S. J., and Ehleringer, J. R.: Water extraction times for plant and soil
629 materials used in stable isotope analysis. *Rapid Commun Mass Sp.*, 20(8), 1317-1321,
630 <https://doi.org/10.1002/rcm.2456>, 2006.

631

632